SIAM Review
Vol. 10, No. 3, July, 1968

THE DYNAMICS OF VARIABLE STARS*

R. F. CHRISTY†

Abstract. Several closely related classes of variable stars—here called Cepheid variables—have long been known, as a result of detailed observation, to be vibrating in a spherically symmetric dilational mode. The purpose of the work described here has been to understand this motion and thereby to be able to apply the extensive data on variable stars in augmenting our knowledge of the stars.

The coupled equations of spherical hydrodynamics and radiation diffusion have been solved numerically as an initial value problem for a variety of stellar models. Unstable models show a growing amplitude of pulsation which ultimately levels off at a stable maximum amplitude of periodic motion. This final motion and the associated large amplitude light variation agree closely with observed variables. Check calculations show that the results are reliable.

The interior dynamics have been examined in order to find the physical cause of the instability and also in order to understand peculiar secondary features of the pulsation. In addition, overtone pulsation in the first radial overtone has been studied. In a few cases, the instability can lead to stable large amplitude periodic motion in either the fundamental or the first overtone, depending on the initial conditions.

Introduction. Since there have recently appeared a number of detailed papers [1]–[6] and extensive reviews [7]–[11] of different aspects of this problem, this paper will merely outline the essentials and will, to a large extent, be in the nature of an introduction to these other published works.

The physical system. For our purposes here, the star is a spherical mass of gas, primarily a mixture of hydrogen and helium, which is contained by its self-gravitation. A temperature gradient and flow of heat from the interior to the surface are maintained by nuclear reactions in the hot central region. The exterior surface is a free surface which radiates the heat arriving from the interior.

The surface temperatures of the Cepheid variables are in the range from 4000°K to 8000°K where the principal gases are primarily unionized and atomic. Below the surface, the temperature rapidly rises to 10000°K where hydrogen ionizes, then to 40000°K where helium becomes completely ionized. The temperature continues to rise as the density increases toward the interior but the density is so low, $\sim 10^{-4}$ to 10^{-8} gm/cc, that the various constituents behave as perfect gases with, however, a specific heat with large peaks near the temperatures where ionization takes place.

The means of heat transport throughout nearly all of the star is radiative diffusion. This is controlled by the mean radiative mean free path or its inverse, the opacity κ. At the surface, the mean free path becomes long as heat is radiated

* Received by the editors July 26, 1967. Presented by invitation at the Symposium on Modern Aspects of Dynamics, sponsored by the Air Force Office of Scientific Research, at the 1967 National Meeting of Society for Industrial and Applied Mathematics, held in Washington, D.C., June 11–15, 1967.

† Alfred P. Sloan Laboratory, California Institute of Technology, Pasadena, California 91109. This work was supported in part by the National Aeronautics and Space Administration under Grant NsG-426 and by the Office of Naval Research under Contract Nonr-220(47).

to infinity. In the region of 10000°K to 20000°K, there is a thin region that is usually unstable to free convection. It appears, however, that the actual heat transport by such convection is usually small in the Cepheid variables and will be neglected in this discussion.

The principal physical complications are found in the opacity κ and in the internal energy of the gas in the regions of partial ionization. The dominant characteristic of κ is a very rapid increase ($\sim T^{12}$) with T up to $T \sim 10^4$ °K, followed by a decrease ($\kappa \sim (\rho/T^3)$) for higher temperatures. This large peak in the opacity leads to a very thin zone near 10^4 °K where the temperature rapidly rises from its photospheric value of $\approx$ 6000°K to about 20000°K. The exceedingly large temperature gradient in this region is the source of the principal difficulties in the treatment of the problem.

The equations of motion. In a Lagrangian system, the mass, $M(r)$, interior to r is the independent space variable. It is

$$M(r) = \int_0^r 4\pi r'^2 \rho(r')\, dr',$$

where $\rho(r)$ is the density. The equation of motion of an element of mass is

$$\frac{\partial^2 r}{\partial t^2} = -\frac{GM(r)}{r^2} - 4\pi r^2 \frac{\partial P(\rho, t)}{\partial M}, \tag{1}$$

where G is the constant of gravitation and P is the pressure.

The radiative diffusion flux $L(r)$ passing radius r is

$$L(r) = -(4\pi r^2)^2 \frac{4\sigma}{3\kappa(\rho, T)} \frac{d(T^4)}{dM}, \tag{2}$$

where σ is the Stefan-Boltzmann constant, $\kappa(\rho, T)$ is the opacity, and T is the temperature. The heat diffusion equation is then

$$T \frac{\partial S(\rho, T)}{\partial t} = -\frac{dL}{dM} + \epsilon(\rho, T), \tag{3}$$

where S is the entropy, and ϵ the nuclear energy source.

At the free surface $M(r) = M$ ($r = R_0$), we use the boundary condition $P = 0$ in the equation of motion. The radiative boundary condition is

$$\left.\frac{d(T^4)}{d\tau}\right|_{\text{surface}} = \left.\frac{T^4}{\text{const.}}\right|_{\text{surface}},$$

where τ is the optical depth. We have used the value $\frac{2}{3}$ for the constant in order to simulate the results of the solution of the transport equation at a free surface.

Because of the rapid increase in density near the core of the star, the amplitude of oscillation becomes very small inside $r = \frac{1}{4}R_0$. This permits the introduction of a rigid boundary at a small but finite inner radius which is outside the sources of stellar energy. There results the boundary condition $\dot{r} = 0$ and $L = L_0$,

the mean luminosity at this inner boundary. This elimination of the central region considerably simplifies the calculations.

The linear calculations. By setting time derivatives equal to zero in (1) and (3), we get equations which, together with the equation of state relating p, ρ, and T, describe the static structure of the stellar envelope (that part of the star outside the central core). This structure is characterized by $\rho \sim T^{3.5}$ over much of the envelope and $T \propto ((1/r) - (1/R_0))$ except in the narrow region of a large temperature gradient. The essentials of the temperature distribution are shown in Fig. 1.

The first treatments of this problem considered the linearized equations resulting from the assumption of small, sinusoidal oscillations about equilibrium. In addition, an adiabatic assumption was made in which the deviations from equilibrium were treated as adiabatic with $\delta p/p = \gamma(\delta\rho/\rho)$.

If the deviation in radius is written $r = r_0(1 + \xi(x, t))$, where $x = r_0/R_0$ and $\xi \sim e^{i\omega t}$, we obtain

$$(4) \qquad \frac{d^2\xi}{dx^2} + (4 - V(x))\frac{1}{x}\frac{d\xi}{dx} + \frac{V(x)}{x^2}\left[\frac{4 - 3\gamma}{\gamma} + \frac{x^3R^3}{\gamma GM(x)}\omega^2\right]\xi = 0,$$

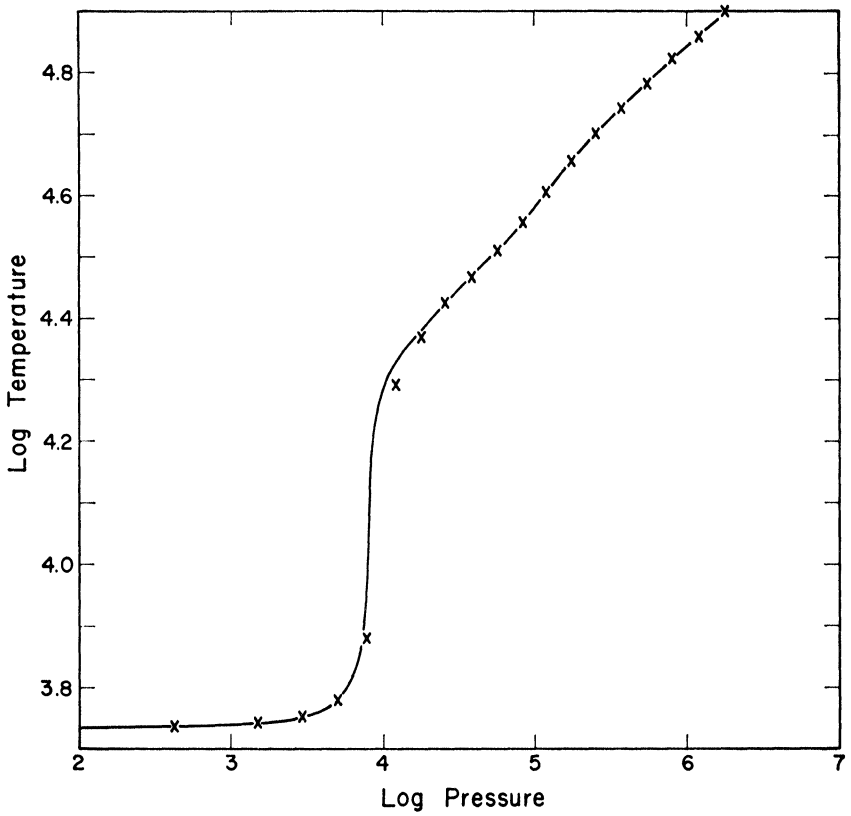

FIG. 1. *The solid curve is the* $\log_{10} T$ *vs.* $\log_{10} P$ *for a fine mass division. The points x are the results of a* 38 *mass zone static model.*

where

$$V(x) = \frac{\rho_0(x)GM(x)}{P_0(x)xR_0}$$

and G is the constant of gravitation.

This equation is an eigenvalue equation for the frequency ω and leads to the amplitude function $\xi(x)$. In addition, it is possible to calculate the rate of change of the oscillation energy W by a perturbation procedure. It is

$$\frac{dW}{dt} = \frac{1}{2}\int_0^M (\gamma - 1)\frac{\delta\rho}{\rho}(\delta\epsilon - \delta(dL/dM))\, dM,$$

which shows that the system can be excited or damped by the variation in nuclear energy production or in the radiation absorption during the oscillation.

For the stars of interest, the amplitude is too small near $x = 0$ (where the nuclear energy is produced) for a significant contribution from $\delta\epsilon$. The dependence of opacity κ on temperature and density throughout much of the envelope leads to a decrease of opacity on compression which implies a damping of vibration. It is only in the surface layers where κ behaves differently and where the adiabatic assumption fails that excitation can arise. We shall see later that the excitation arises in the region of partial ionization of helium and in the region of the steep temperature "front" where hydrogen is partly ionized. This temperature front is not well-treated in the linear theory since the amplitude is there locally so large. A better picture of the variation in this region is to regard it as a moving front which oscillates back and forth in the star.

The nonlinear method. In order to treat better the surface regions of very large relative amplitude and to study the behavior of an actual large amplitude variable star, nonlinear calculations were initiated. In this method, the envelope is divided into a series of spherical shells of carefully chosen relative mass. The equations of motion then become coupled differential equations for the motion and temperature variation of these mass shells. These equations are then integrated numerically in time from some initial conditions. The radiation diffusion equation was treated by an implicit differencing method to guarantee stability and the hydrodynamics was treated by an explicit procedure in which the time step was controlled by the Courant condition, which, for stability reasons, restricts Δt to a value less than the time for sound to cross a zone. The exact equation of state and opacity law were used in tabular form.

The major problem in this calculation results from the steep temperature front which coincides with an important source of excitation in the star. Any attempt to use sufficiently fine zones to give an adequate description of this region leads to such short time steps that the calculation became impractical, requiring about one hour, on an IBM 7094, for one period of vibration. After considerable study, it was found that a description in terms of thick zones (considerably thicker than the front itself) could be used provided a transparency average of opacity of neighboring zones was used $2/\bar{\kappa} \approx (1/\kappa_1) + (1/\kappa_2)$. Actually, a somewhat more complicated average of this type was used which

was constructed to agree with exact integrations of the equation of heat flow on both sides of the front even for large differences of temperature [8]. The points marked x in Fig. 1 show that this procedure was successful in integrating through the front with very few steps. This procedure is satisfactory only if the vibration amplitude is large enough so that the front crosses several zones in one period. For very small amplitude, the procedure is, in general, not precise and the results depend to some extent on the exact location of the front with respect to the coarse zones. In the problems of interest, the large amplitude condition was satisfactorily fulfilled with a description in terms of about 40 zones for the entire envelope. This permitted two time steps per second and about one period of vibration in one minute on an IBM 7094. The general temperature distribution in an equilibrium model is shown in Fig. 2. The zones were thin near the stellar surface and increased steadily (by about a factor 1.4 in mass per zone) toward the interior. This permitted considerable detail (about 15 zones) in the regions near the surface which cause the excitation; about 15 zones in the region of important dissipation and about 10 further zones in the region of very small amplitude leading to the rigid boundary.

Temporal behavior of the system. The system of equations was integrated numerically by first integrating the corresponding equilibrium equations in order to arrive at a static model for the initial condition of the dynamics. The usual method of initiating the dynamics was to superpose on the static model some prescribed run of $\dot{r}(M)$. These initial velocities were usually chosen so as

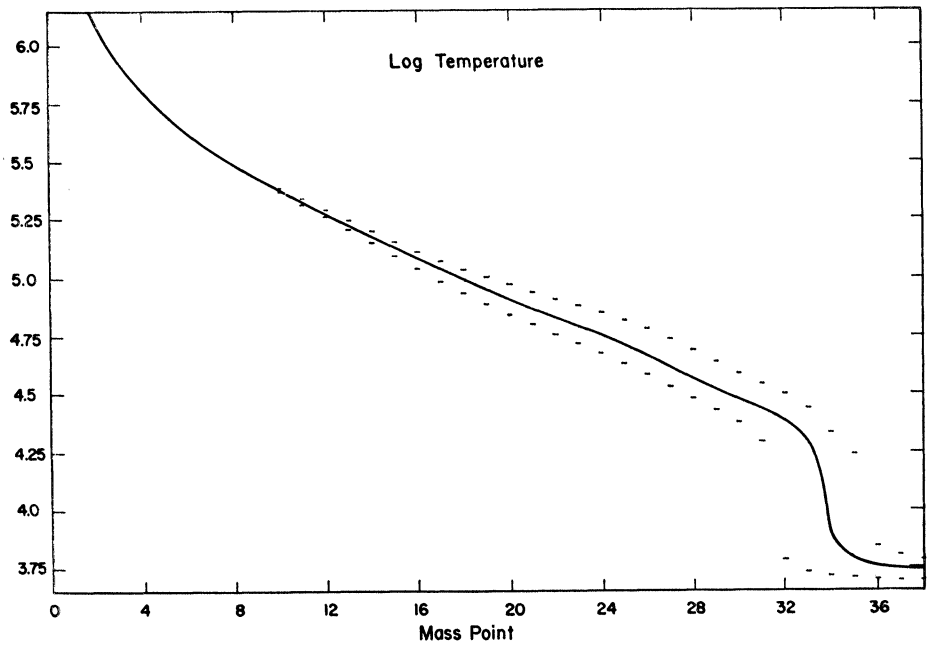

FIG. 2. *The* $\log_{10} T(°K)$ *of the mass zones of a static model. The amplitude of the final variation is shown by the dashed line.*

to approximate the velocities in a linear mode of vibration and with a large enough amplitude to minimize the time for the nonlinear integrations.

Following initiation in this way, if the velocity distribution was well chosen, there results an approximately periodic vibration of the system which was found to slowly decay in amplitude, for a stable model, or slowly grow in amplitude for an unstable model. Together with the slow growth in amplitude, the solution also approximates better and better to periodicity as the unwanted modes contaminating the principal mode (usually the fundamental) slowly decay. After some growth in amplitude (usually at least quadrupling the energy of vibration), the amplitude approaches an asymptotic limit characterizing the physical system (see Fig. 3). In this limit, the motion is nonsinusoidal throughout the star, even where the amplitude is small. Near the surface, the material velocities exceed sonic by a factor of 2 to 4 and shock waves may, in some cases, be seen. They were treated by the Von Neumann-Richtmyer artificial viscosity method.

The model envelopes considered here are characterized by parameters giving the mass M, radius R_0, surface temperature T_e (or mean luminosity L_0) and a chemical composition specifying the ratio of helium to hydrogen. In this parameter space, the region of instability has been approximately delineated by numerous integrations with differing models. In addition, the nature of the non-

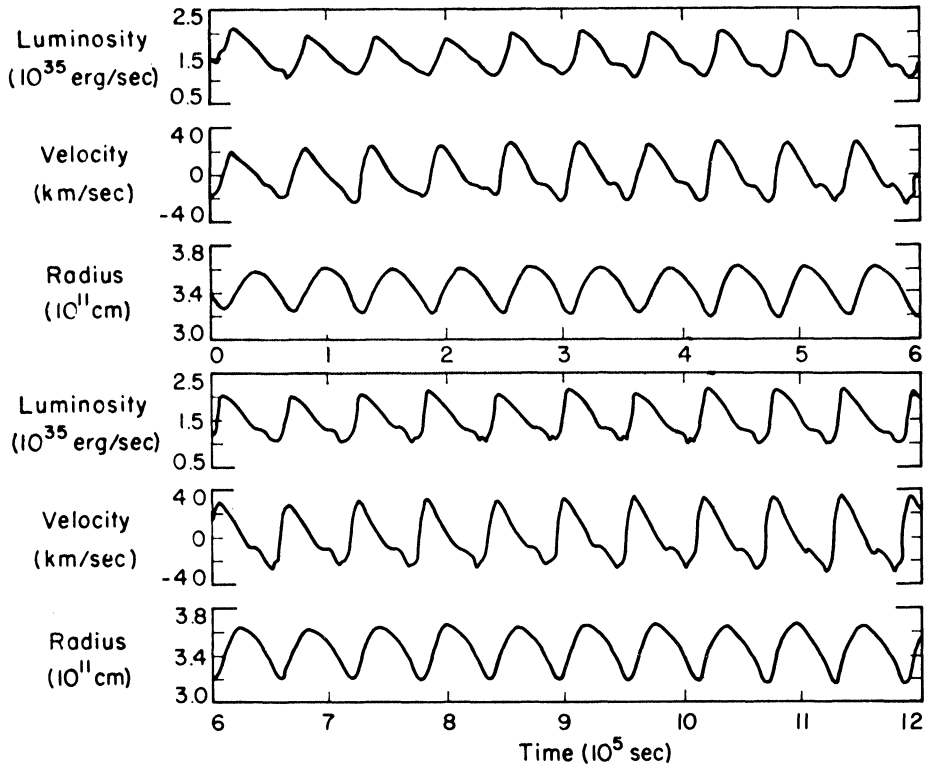

FIG. 3. *The growth of amplitude for the first* 20 *periods of a model. The emerging luminosity, surface velocity, and photospheric radius are shown.*

linear motions has been studied. This has permitted a better understanding of some aspects of the problem and also the determination of some of the physical parameters by fitting calculated models to observation.

The cause and limitation of instability. In order to explore the sources of excitation and dissipation, P-V diagrams were drawn for each zone in a typical example. The diagrams for a few representative zones are shown in Fig. 4. Zone 22 is typical of the dissipating region where the motion is quasi-adiabatic. Zones

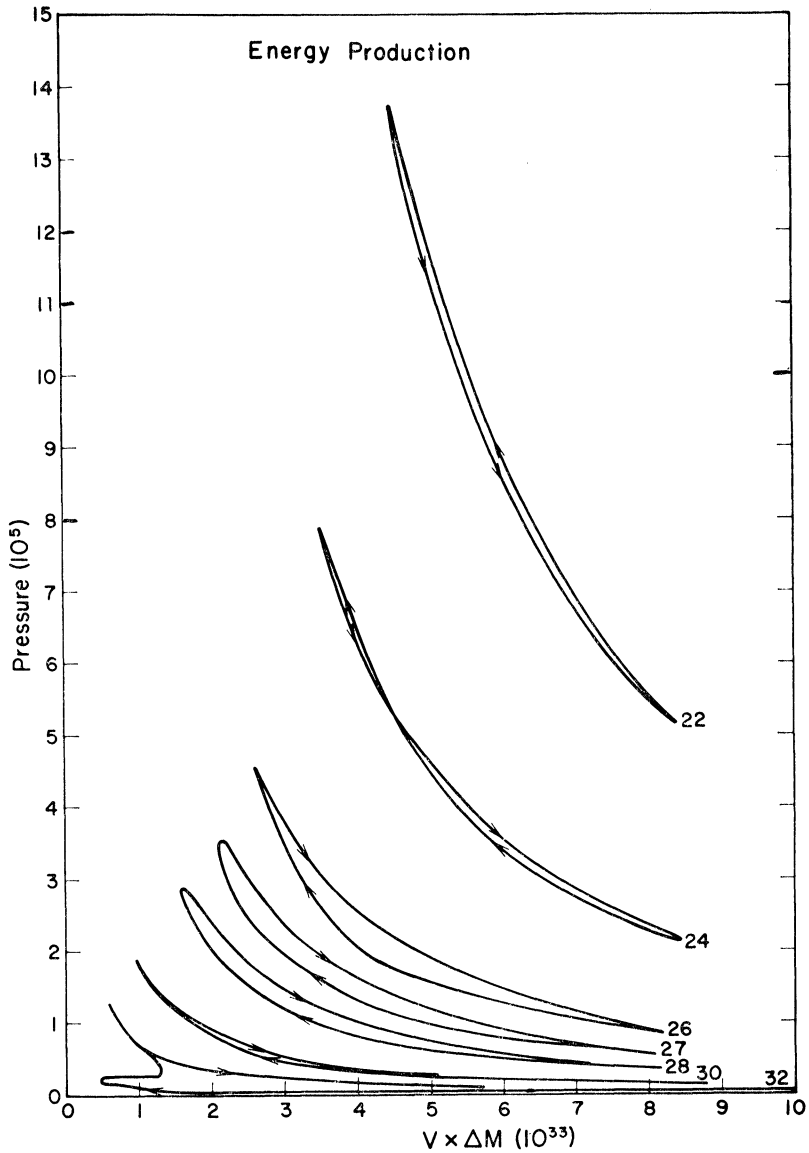

FIG. 4. *P-V diagrams for mass zones* 32, 30, 28, 27, 26, 24, *and* 22. *The abscissa is the total volume occupied by each mass zone.*

26, 27 and 28 are typical of the excitation found in the region of partial helium ionization near 40000°K. Zone 32 is typical of the excitation in the region of the steep front which moves over several zones and gives a strong excitation near 10000°K. The net effects of all zones are shown in Fig. 5. The dissipation in the zones 10 to 25 has already been explained in terms of the decrease in opacity and consequent increased heat flow when compressed. The excitation in the helium zone is due to two causes—a peculiar behavior of the opacity law and the very high heat capacity which keeps this region relatively cooler on compression and leads to heat absorption at that phase. The excitation in the hydrogen zone is associated with the strong increase of opacity, leading to trapping the heat flux on compression.

The limitation of amplitude is shown in Fig. 6 where the total excitation and total dissipation are shown as a function of amplitude—the amplitude was artificially carried to a value in excess of the true limiting amplitude (where the difference between the excitation and dissipation vanishes) by inserting a growth factor into the calculation. It appears that the principal levelling off is in the excitation due to the helium zone. It was found by further investigation that this was associated with the amplitude becoming so large in this zone that the duration of outward acceleration became very small and a very large pressure peak developed. This, in turn, made the temperature rise so far that the opacity decreased and the excitation was diminished in the helium zone.

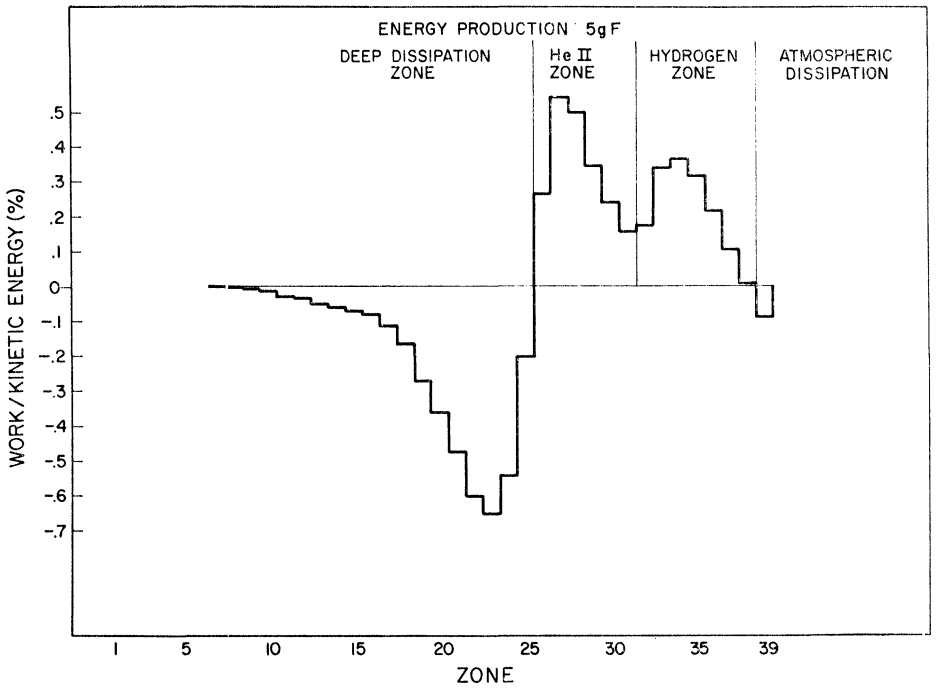

FIG. 5. *The energy production and dissipation for all zones. Positive ordinates are work production and negative ordinates are dissipation.*

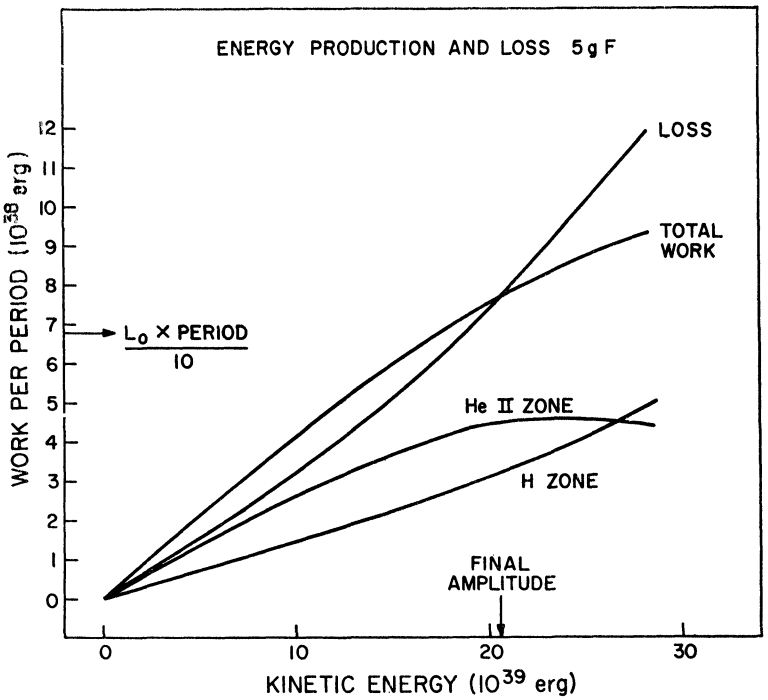

FIG. 6. *The variation with amplitude of the work production in different regions and of the total dissipation. The amplitude is measured by the total kinetic energy of the motion at its peak.*

Because the excitation arises in the layers of partial hydrogen and helium ionization which are quite near the stellar surface, we can understand why the excitation is confined to a narrow range of surface temperatures (5000°K–7000°K). For hotter stars, the zones of partial ionization are too thin and have too little heat capacity to be able to act effectively. For cooler stars, the zones are so thick that they tend to act nearly adiabatically. In addition, the behavior in the hydrogen zone is complicated by the development of convective heat transport in the cooler stars. Until now, the calculations have not been able to treat this form of heat flow and the behavior of cool envelopes is still not understood.

Overtone behavior. One of the interesting nonlinear results relates to the excitation of the first radial overtone. In the linear calculations, both the fundamental, the first radial overtone and higher overtones are strongly excited in the same instability region.

Observed stars, on the other hand, show motion in the fundamental and, in certain cases, motion in the first overtone but only on the high temperature side of the instability region.

The nonlinear models showed a behavior similar to the observations. For a high ratio of luminosity to mass, the whole width (in mean surface temperature)

of the instability region is occupied by models which, at large amplitude, persist in vibration in the fundamental mode. For a low ratio of luminosity to mass, the width of the instability region is occupied by models which, at large amplitude, persist in vibration in the first overtone. For intermediate ratios of luminosity to mass, the high surface temperature models show persistent vibration in the first overtone while the lower surface temperature models show persistent vibration in the fundamental mode.

The dividing line (in mean surface temperature) between these types is of special interest but could only be explored somewhat crudely. Nevertheless, certain models were found such that, if initiated at intermediate amplitude in the fundamental, the fundamental would grow and contamination of the first overtone would decay. On the other hand, if the same model was initiated at intermediate amplitude in the first overtone, the latter would grow and contamination due to the fundamental would decay. In other words, for these models, the final large amplitude vibration depends on the history of the system.

This nonlinear behavior of the calculation is quite consistent with observation of the stars and served as the basis of a determination of stellar luminosity [5] by matching calculations to observation. Nevertheless, a deeper understanding is still lacking of the reasons the system prefers one mode or the other.

Secondary nonlinear effects. Certain stars show, in addition to the principal peak in luminosity, a secondary smaller peak somewhat later in the cycle. When it was realized that this secondary peak also appears in the observed surface velocities in several observed cases, an effort was made to find models which showed this effect and to investigate its cause. The cause was revealed by two different studies. In Fig. 7 are shown velocities for all zones in a 42 zone model when vibrating at constant amplitude in the fundamental. The zeros of successive curves are displaced and, in addition, the scale is progressively enhanced from zone 42 (the outside) to zone 2 (the inside) by a factor reaching 1600. The secondary peak in outward velocity appears in the surface zone at phase 0.4 delayed by about 0.4 periods after the main phase of outward acceleration at phase 0.0. The motion in the intermediate zones (near 30) shows some approximation to sinusoidal behavior but in the deep interior (zones 2 to 10) the motion consists of a brief impulse each period. The cause of this impulsive motion at the center near phase 0.5 has been traced to the high-pressure signal associated with the outward acceleration peak some half period earlier at phase 0.0. This is fairly clear in the figure where the signal can be traced inward. It has also been checked in a model by following the motion from initiation where the impulsive behavior near the center first appears after the first high-pressure peak in the outer layers. The signal can be further traced outward again from the center until it reaches the surface and leads to the secondary velocity peak and outward acceleration which can be described as an echo of the principal outward acceleration peak about 1.4 periods earlier.

The delay of the secondary peak (here 1.4 periods) depends on the ratio of the time for sound to traverse the envelope to the period of the motion. This

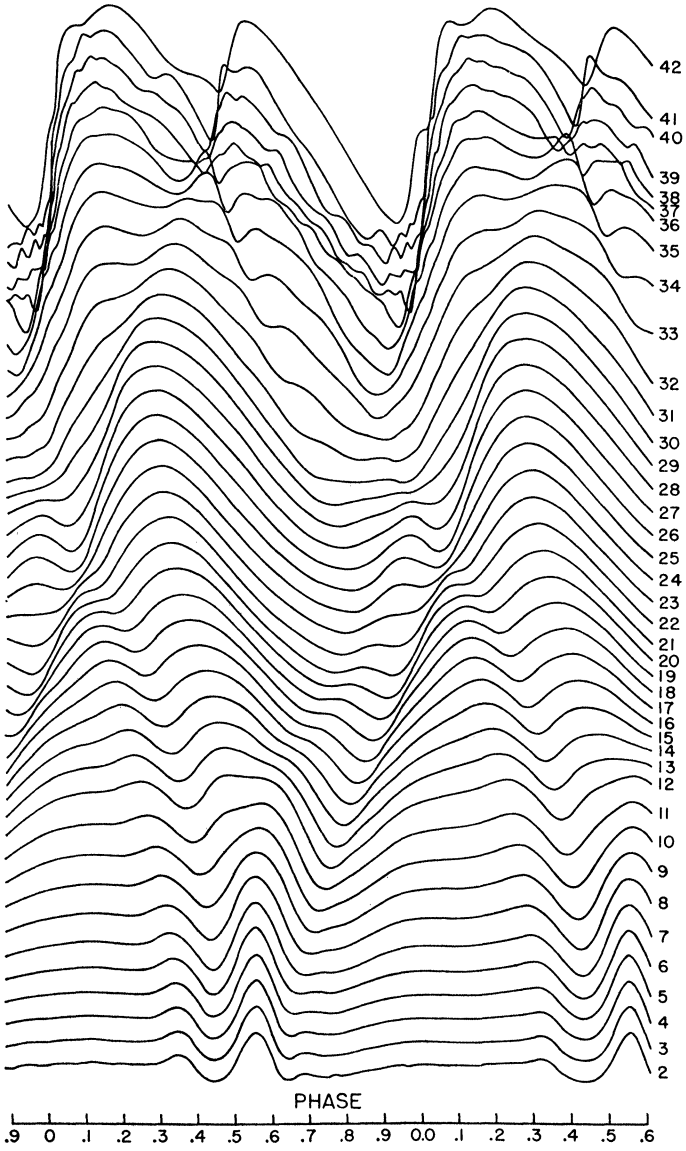

FIG. 7. *Velocities of all zones in a 42 zone model. Zone 42 is the outermost and zone 2 the innermost. The actual amplitude at zone 42 is ±27 km/sec. The scale of the inner zones is progressively enhanced and the actual amplitude at zone 2 is ±0.007 km/sec.*

ratio, in turn, depends on the structure of the envelope and is closely determined by the run of the function $V(x)$ in (4).

In addition to interest in understanding the nonlinear features, the ability to calculate a feature of this kind can be used to determine the basic parameters of the model that agrees with the observed star. From (4), we see that for a given envelope structure (specified by $V(x)$) the period $\propto R^{3/2}/M^{1/2}$. In addition,

determining the delay of the echo determines the run of $V(x)$ and thereby determines M/R on which the echo delay is principally dependent. The two measurements then give both M and R. If these are combined with measurements of the mean surface temperature, the mean luminosity L_0 is given. In this way, the nonlinear calculations can be used to determine all of the significant parameters of the star.

Conclusion. Nonlinear dynamical calculation of stellar pulsation has been used to reveal the physical explanation of the behavior of the system. In addition, the calculation and understanding of nonlinear aspects of behavior have been used to determine masses, radii, and luminosities of stars.

A wealth of different features are known in actual Cepheid-type variable stars and some of these features are still unexplored. The possible existence of persistent large amplitude mixtures of different overtones is suggested by observation but not yet studied. A related question is, "Are there other forms of nonperiodic solutions?" In one case, the large amplitude motion led ultimately to a motion where alternate periods showed larger and smaller amplitude—a double periodicity effect. Similar behavior is seen in some stars but it is still not explored or understood. In one example, such a strong outward shock developed each period that the outermost mass zones were successively driven off from the star. Such possible mass ejection resulting from pulsation is of great interest but is, as yet, quite unexplored by any reliable calculations. Finally, the instability of low-surface temperature models where free convection is important is still unexplored although variable stars in this region are known to exist.

REFERENCES

[1] N. Baker and R. Kippenhahn, *The pulsations of models of δ Cephei stars*, Zs. f. Astrophys., 54 (1962), pp. 114–151.

[2] J. P. Cox, *On second helium ionization as a cause of pulsational instability in stars*, Astrophys. J., 138 (1963), pp. 487–536.

[3] N. Baker and R. Kippenhahn, *The pulsations of models of delta Cephei stars II*, Ibid., 142 (1965), pp. 868–889.

[4] R. F. Christy, *The calculation of stellar pulsation*, Rev. Modern Phys., 36 (1964), pp. 555–571.

[5] ———, *A study of pulsation in RR Lyrae models*, Astrophys. J., 144 (1966), pp. 108–179.

[6] A. N. Cox, R. R. Brownlee and D. D. Eilers, *Time dependent method for computation of radiation diffusion and hydrodynamics*, Ibid., 144 (1966), pp. 1024–1037.

[7] R. F. Christy, *Pulsation theory*, Annual Review of Astronomy and Astrophysics, vol. 4, L. Goldberg, ed., Annual Reviews Inc., Palo Alto, California, 1966, pp. 353–392.

[8] ———, *Computational methods in stellar pulsation*, Methods in Computational Physics, B. Alder, ed., vol. 7, Academic Press, New York, 1966, pp. 191–218.

[9] S. A. Zhevakin, *Physical basis of the pulsation theory of variable stars*, Annual Review of Astronomy and Astrophysics, vol. 1, L. Goldberg, ed., Annual Reviews Inc., Palo Alto, California, 1963, pp. 367–400.

[10] R. F. Christy, *Non-linear calculations for pulsating stars*, Aerodynamic Phenomena in Stellar Atmosphere, R. N. Thomas, ed., Academic Press, New York, 1967, pp. 105–156.

[11] J. Cox, *The linear theory: Initiation of pulsational instability in stars*, Ibid., pp. 3–72.